

Space-time evolution of ultra-relativistic heavy ion collisions and hadronic spectra

B. K. Patra^{a1}, Jan-e Alam^a, Pradip Roy^b, Sourav Sarkar^a and Bikash Sinha^{a,b}

a) Variable Energy Cyclotron Centre, 1/AF Bidhan Nagar, Kolkata 700 064, India

b) Saha Institute of Nuclear Physics, 1/AF Bidhan Nagar, Kolkata 700 064, India

Abstract

The space-time evolution of the hot and dense matter formed after the collisions of heavy nuclei at ultra-relativistic energies is investigated using (3+1) dimensional hydrodynamical models. The effects of the spectral shift of the hadronic properties are incorporated in the equation of state (EOS) of the evolving matter. In-medium shift of hadronic properties are considered for Quantum Hadrodynamics (QHD) and universal scaling scenarios. It is found that the EOS for the hadronic matter for universal scaling of hadronic masses (except pseudoscalar) is similar to the recent lattice results. We observe that the space-time volume of the hadronic matter at the freeze-out is considerably different from the one when medium effects on the hadrons are ignored. The sensitivity of the results on the initial radial velocity profile is investigated. The transverse mass spectra of pions and protons of NA49 collaboration are analyzed.

1 Introduction

One of the main motivations to study the nucleus-nucleus collisions at ultra-relativistic energies is to create a very hot and dense system of strongly interacting matter, a situation conducive for the formation of Quark Gluon Plasma (QGP) [1]. It is not easy, however, to obtain information about the early stage of this matter because of the very short lifetime of the dense system. Electromagnetically interacting particles (photons and lepton pairs) are considered to be the ideal probes for the early state of the matter. On the other hand, observations through the transverse mass (m_T) spectrum of the hadrons provide valuable informations about the situation when the thermal system freezes out [2, 3, 4, 5, 6], *i.e.* the stage when the system

¹Present Address: Saha Institute of Nuclear Physics, 1/AF Bidhan Nagar, Kolkata 700 064

disassembles to individual hadrons. Thus the study of the hadronic spectra gives snapshots of the later stages of the nuclear collision dynamics.

It has been emphasized recently that the properties of the hadrons will be modified due to its interactions with the particles in the thermal bath. It is also worth emphasizing here that as yet it has not been possible to explain the enhanced dilepton production measured by the CERES/NA45 collaborations [7] in the low invariant mass region (below the ρ -peak) without the in-medium modifications of the vector mesons [8]. We have recently analyzed [9] the WA98 photon data [10] by incorporating the in-medium modifications of hadrons. In the light of these observations we study the hadronic spectra in a scenario where the hydrodynamic evolution contains the in-medium modifications of hadrons through the parametrization of the equation of state (EOS). In particular we will show here that the NA49 [11] hadronic spectra can be explained by the same initial and freeze-out conditions with the EOS which explain the photon and dilepton data at CERN SPS energies. We consider two possible scenarios: (i) nucleus + nucleus \rightarrow QGP \rightarrow hadrons and (ii) nucleus + nucleus \rightarrow excited hadronic matter \rightarrow hadrons (but the properties of hadrons in the thermal bath are different from the vacuum due to its interaction with the particles in the thermal bath), to investigate the evolution of the matter formed after the collisions.

In the next section we review the hydrodynamical model and the EOS used in the present work. In section 3 we present the results of our calculations and section 4 is devoted to summary and discussions.

2 The Single-particle Spectra in the Hydrodynamical Model

We will assume that the produced matter reaches a state of local thermodynamic equilibrium after a proper time, $\tau_i \sim 1$ fm/c [12]. The system continues to expand in space and time till the freeze-out undergoing a phase transition to the hadronic matter in the process, if QGP is formed initially. The conversion of thermal energy of the system into the collective flow continues as long as collisions are sufficiently frequent. Eventually the density of the particles decreases and correspondingly their

mean free path increases. When the mean free path becomes of the order of the size of the system, hadrons act as non-interacting free particles. The detailed description of this decoupling transition, or freeze-out, is complicated. A simple algorithm is obtained if one assumes that the break-up occurs when the temperature drops down to a given decoupling temperature T_F ; this temperature, which is typically of the order of the pion mass, defines a space-time surface $T(r, t) = T_F$, usually referred to as the freeze-out surface (FS), on which the system ceases to behave collectively. A fluid element which crosses this surface liberates particles which, in the rest frame of the fluid element, have a thermal distribution at a temperature T_F . Knowing the velocity of the fluid element on the decoupling surface, one can then determine the momentum distribution of the final particles. The observed momentum distribution will thus be characterized by the temperature and collective velocity of the system at the FS. For given initial conditions and EOS we solve the hydrodynamical equations to obtain the FS, determined by the condition, $T(\tau, r) = T_F$.

The expansion of the system is described by the energy-momentum conservation of an ideal fluid :

$$\partial_\mu T^{\mu\nu} = 0; \quad T^{\mu\nu} = (\epsilon + P)u^\mu u^\nu + g^{\mu\nu}P \quad (1)$$

where ϵ is the energy density, P is the pressure measured in the frame co-moving with the fluid, and u^μ is the fluid four-velocity.

With the assumption that the system undergoes a boost-invariant longitudinal expansion along the z axis [12] and a cylindrically symmetric transverse expansion the hydrodynamic Eqs. 1 reduce to

$$\partial_\tau T^{00} + \frac{1}{r}\partial_r(rT^{01}) + \frac{1}{\tau}(T^{00} + P) = 0 \quad (2)$$

and

$$\partial_\tau T^{01} + \frac{1}{r}\partial_r[r(T^{00} + P)v_r^2] + \frac{1}{\tau}T^{01} + \partial_r P = 0 \quad (3)$$

where $u^\mu = \gamma(t/\tau, \vec{v}_r, z/\tau)$

Eqs. (2) and (3) are solved by the relativistic version of the flux corrected transport algorithm [13] with the following initial energy density profile,

$$\epsilon(\tau_i, r) = \frac{\epsilon_0}{1 + \exp[(r - R_A)/\delta]}. \quad (4)$$

where R_A is the nuclear radius and δ is the surface thickness parameter. We have taken $\delta = 1/2$ in our calculations. We will study the sensitivity of the flow with the following two kinds of initial velocity profile [14, 15],

$$v_r(\tau_i, r) = v_0 \frac{r}{R_A} \quad (5)$$

and [13]

$$v_r(\tau_i, r) = v_0 \left[1 - \frac{1}{1 + \exp[(r - R_A)/\delta]} \right] \quad (6)$$

The FS, which is required as an input to evaluate the single particle spectra is obtained by solving the Eqs. (2) and (3) with the initial conditions (4) and (5) (or eq.6) for a given EOS.

The single particle transverse momentum distribution in the hydrodynamical model is given by the well-known Cooper-Frye formula [16],

$$E \frac{dN}{d^3p} = \frac{g}{(2\pi)^3} \int_{\sigma} f(r, p) p^{\mu} d\sigma_{\mu}, \quad (7)$$

where $f(r, p)$ is the Boltzmann distribution (quantum statistical effects are neglected here)

$$f(r, p) = \exp[-(p \cdot u - \mu)/T]. \quad (8)$$

T , μ and u^{μ} are the temperature, chemical potential and four-velocity of the fire-cylinder respectively. The three dimensional space-time surface σ , whose surface elements are specified in terms of the four vector $d\sigma^{\mu} = (d^3r, dt dS)$, is determined by the freeze-out condition, $T(\tau, r) = T_F$ as mentioned before. For a system with cylindrical symmetry and boost invariance along the longitudinal direction the single particle momentum (p_T) distribution is given by [14, 17, 18],

$$\begin{aligned} \left(\frac{dN}{dy p_T dp_T} \right)_{y=0} &= \frac{g}{\pi} \int_{\sigma} r dr \tau_F(r) \\ &\left\{ m_t I_0 \left(\frac{p_T \sinh y_t}{T} \right) K_1 \left(\frac{m_t \cosh y_t}{T} \right) \right. \\ &\left. - \left(\frac{\partial \tau_F}{\partial r} \right) p_T I_1 \left(\frac{p_T \sinh y_t}{T} \right) K_0 \left(\frac{m_t \cosh y_t}{T} \right) \right\} \quad (9) \end{aligned}$$

where $\tau_F(r)$ refers to the freeze-out time which, in general, depends on r and y_t is the transverse rapidity.

2.1 Equation of state

The set of hydrodynamic eqs. (2) and (3) are not closed by itself; the number of unknown variables exceeds the number of equations by one. Thus a functional relation between any two variables is required so that the system becomes deterministic. The most natural course is to look for such a relation between the pressure P and the energy density ϵ . Under the assumption of local thermal equilibrium, this functional relation between P and ϵ is the EOS. Obviously, different EOS's will govern the hydrodynamic flow quite differently and as far as the search for QGP is concerned, the goal is to look for distinctions in the observables due to the different EOS's (corresponding to the novel state of QGP vis-a-vis that for the hadronic matter). It is thus imperative to understand in what respects the two EOS's differ and how they affect the evolution in space and time.

A physically intuitive way of understanding the role of the EOS in governing the hydrodynamic flow lies in the fact that the velocity of sound $c_s^2 = (\partial P/\partial \epsilon)_s$ sets an intrinsic scale in the hydrodynamic evolution. One can thus write a simple parametric form for the EOS: $P = c_s^2(T)\epsilon$. Clearly, inclusions of interactions may drastically alter the value of c_s^2 . In the present work MIT bag model equation of state is assumed for the QGP where the energy density and pressure are given by

$$\epsilon_Q = g_Q \frac{\pi^2}{30} T^4 + B, \quad (10)$$

and

$$P_Q = g_Q \frac{\pi^2}{90} T^4 - B. \quad (11)$$

The effective degrees of freedom in QGP, $g_Q = 37$ for two flavours. The entropy density s_Q is given by $s_Q = 2g_Q(\pi^2/45)T^3$.

As the hydrodynamic expansion starts, the QGP begins to cool until the temperature drops down to the critical temperature T_c . At this instant, the phase transition to the hadronic matter starts. Assuming that the phase transition is a first-order one, the released latent heat maintains the temperature of the system at the critical temperature T_c , even though the system continues to expand. The cooling due to expansion is compensated by the latent heat liberated during the process. We neglect the scenarios of supercooling or superheating and any other plausible

explosive events. This process continues until all the matter has converted to the hadronic phase with the temperature remaining constant at $T = T_c$. From then on, the system continues to expand, governed by the EOS of the hot hadronic matter till the freeze-out temperature T_F at the proper time τ_F . Thus the appearance of the so called mixed phase at $T = T_c$, when QGP and hadronic matter co-exist, is a direct consequence of the first order phase transition. Apart from the role in QGP diagnostics, the possibility of the mixed phase affects the bulk features of the evolution process also.

In the hadronic phase one must consider the effect of the presence of heavier particles and the change in their masses due to finite temperature effects. The ideal limit of treating the hot hadronic matter as a gas of pions originated from the expectation that in the framework of local thermalization the system would be dominated by the lowest mass hadrons while the higher mass resonances would be Boltzmann suppressed. Indirect justification of this assumption comes from the experimental observation in high energy collisions that most of the secondaries are pions. Nevertheless, the temperature of the system is higher than m_π during a major part of the evolution and at these temperatures the suppression of the higher mass resonances may not be complete. It may therefore be more realistic to include higher mass resonances in the hadronic sector, their relative abundances being governed by the condition of (assumed) thermodynamic equilibrium. We assume that the hadronic phase consists of π , ρ , ω , η , a_1 mesons and nucleons. The nucleons and heavier mesons are expected to play an important role in the EOS particularly, in a scenario where mass of the hadrons decreases with temperature.

The energy density and pressure for such a system of hadrons are given by

$$\epsilon_H = \sum_{h=\text{mesons}} \frac{g_h}{(2\pi)^3} \int d^3p E_h f_{BE}(E_h, T) + \frac{g_N}{(2\pi)^3} \int d^3p E_N f_{FD}(E_N, T) \quad (12)$$

and

$$P_H = \sum_{h=\text{mesons}} \frac{g_h}{(2\pi)^3} \int d^3p \frac{p^2}{3 E_h} f_{BE}(E_h, T) + \frac{g_N}{(2\pi)^3} \int d^3p \frac{p^2}{3 E_N} f_{FD}(E_N, T) \quad (13)$$

where the sum is over all the mesons under consideration and N stands for nucleons. The in-medium mass of the hadrons (H) enters through the relation,

$E_H = \sqrt{p^2 + m_H^{*2}}$ (the asterisk denotes the effective mass in the medium). The entropy density is then given by

$$s_H = \frac{\epsilon_H + P_H}{T} \equiv 4a_{\text{eff}}(T) T^3 = 4\frac{\pi^2}{90} g_{\text{eff}}(m^*(T), T) T^3 \quad (14)$$

where g_{eff} is the effective statistical degeneracy. Thus, we can visualize the finite mass of the hadrons having an effective degeneracy $g_{\text{eff}}(m^*(T), T)$. We consider the effects of in-medium mass on the EOS both for the universal scaling scenario [19] and the Quantum Hadrodynamic (QHD) scenario. According to the universal scaling scenario the hadronic masses (except pseudoscalars) approaching zero near the critical temperature as follows [19],

$$m_H^*/m_H = (1 - T^2/T_c^2)^\lambda \quad (15)$$

Results for various values of the exponent λ will be discussed below. For a detailed discussions on the in-medium masses of hadrons in QHD interaction we refer to [20, 21, 22]. The temperature dependence of the mass of nucleon (m_N^*), ρ (m_ρ^*) and ω (m_ω^*) in QHD are parametrized as follows:

$$m_N^* = m_N \left[1 - 0.0264 \left(\frac{T(\text{GeV})}{0.16} \right)^{8.94} \right]. \quad (16)$$

$$m_\rho^* = m_\rho \left[1 - 0.127 \left(\frac{T(\text{GeV})}{0.16} \right)^{5.24} \right] \quad (17)$$

$$m_\omega^* = m_\omega \left[1 - 0.0438 \left(\frac{T(\text{GeV})}{0.16} \right)^{7.09} \right]. \quad (18)$$

The effective mass of the a_1 meson, $m_{a_1}^*$ has been estimated from m_ρ^* by using Weinberg's sum rule [23].

3 Results

In Fig. 1 the variation of the effective degeneracy (the co-efficient of ϵ/T^4 differs from the effective degeneracy by a multiplicative factor of $\pi^2/30$) is plotted as a function of temperature. The rapid increase of the effective degeneracy near the critical temperature as per lattice QCD calculations [24] is reasonably well described when the effective masses vary according to the eq.(15) (see also [25]).

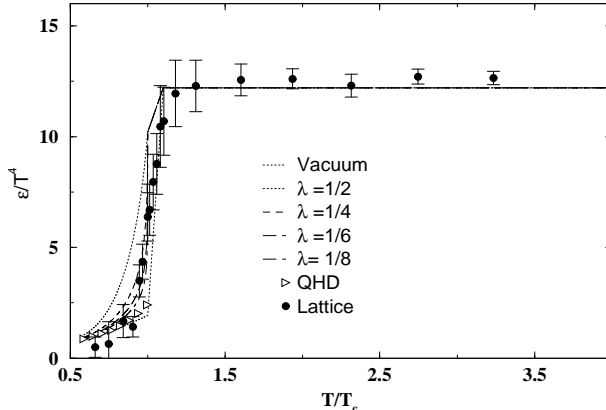


Figure 1: The energy density ϵ in unit of T^4 for various equations of state used in the present work are plotted as a function of temperature in unit of the critical temperature, T_c . The filled circles denote the lattice results [24]. The dashed line indicates results with vacuum masses.

We solve the following equation to estimate the initial temperature,

$$\frac{dN_\pi}{dy} = \frac{45\zeta(3)}{2\pi^4} \pi R_A^2 4a_{\text{eff}}(T_i) T_i^3 \tau_i \quad (19)$$

where $a_{\text{eff}}(T_i) = (\pi^2/90) g_{\text{eff}}(m^*(T_i), T_i)$. The change in the expansion dynamics as well as the value of the initial temperature due to medium effects enters the calculation through the effective statistical degeneracy.

	QGP	vacuum mass	QHD	Scaling $T_c=200$ MeV
dN/dy	T_i (MeV)	T_i (MeV)	T_i (MeV)	T_i (MeV)
700	196	245	220	205

Table I: Initial temperatures for QGP and hadronic initial states.

We consider Pb + Pb collisions at CERN SPS energies. Taking $dN_\pi/dy = 700$ for Pb + Pb collisions and $\tau_i = 1$ fm/c, Eqs. (14) and (19) are solved self consistently to get the initial temperatures for different mass variation scenarios shown in Table I. For a given dN/dy and τ_i the value of T_i is higher in case of vacuum masses (smaller a_{eff}) compare to the universal scaling scenario (higher a_{eff}).

Next we consider the constant energy density contours at the FS. The value of T_F is taken as 120 MeV in the present calculations. Eqs. (4) and (5) are used for the initial energy density and velocity profiles respectively. In case of QGP formation

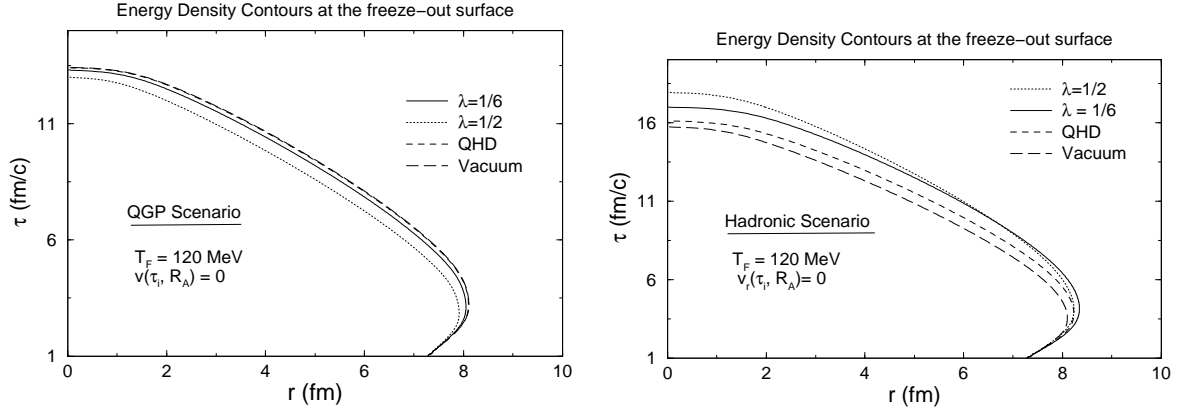


Figure 2: Constant energy density contours at the FS (in $r - \tau$ plane) for initial velocity profile of Eq. 5 with $v_0 = 0$. Left (Right) : QGP (hadronic) initial state.

the initial energy density is $2.6 \text{ GeV}/\text{fm}^3$ corresponding to an initial temperature of 196 MeV . In this case the in-medium effects on the hadronic phase formed after the phase transition is taken into account. The energy density at the freeze-out point, ϵ_F ($\propto a_{eff}(T_F)T_F^4$) is different for different hadronic model. ϵ_F is larger for the universal scaling scenario with $\lambda = 1/2$ compared to the case of the hadronic gas with vacuum masses, because for a given T_F , a_{eff} is larger in the former case. As a consequence of this the FS is smaller in universal scaling scenario compared to the vacuum scenario. This is demonstrated in the left panel of fig. 2. The FS corresponding to QHD and the vacuum are indistinguishable because of the small medium effects in QHD especially at the late stage of the evolution, where the temperature is lower. In the right panel of fig. 2 we display the constant ϵ_F surfaces for hadronic initial state. The velocity of sound in case of universal scaling is smaller than the scenario when medium effects are ignored. As a result the FS for the universal scaling scenario is larger (for a given T_F) as compared to the vacuum mass scenario, because of the slower cooling of the system in the former case.

In fig. 3 the results for non-zero initial radial velocity on the surface of the cylinder is depicted. Because of the rapid expansion of the system the freeze-out surface is smaller (*i.e.* the life time is shorter) in this case as compared to the case where the initial radial velocity is zero at the surface. However, the qualitative shape of the curves are same as before.

Fig. 4 shows the FS when a different initial velocity profile, Eq. 6 is used with

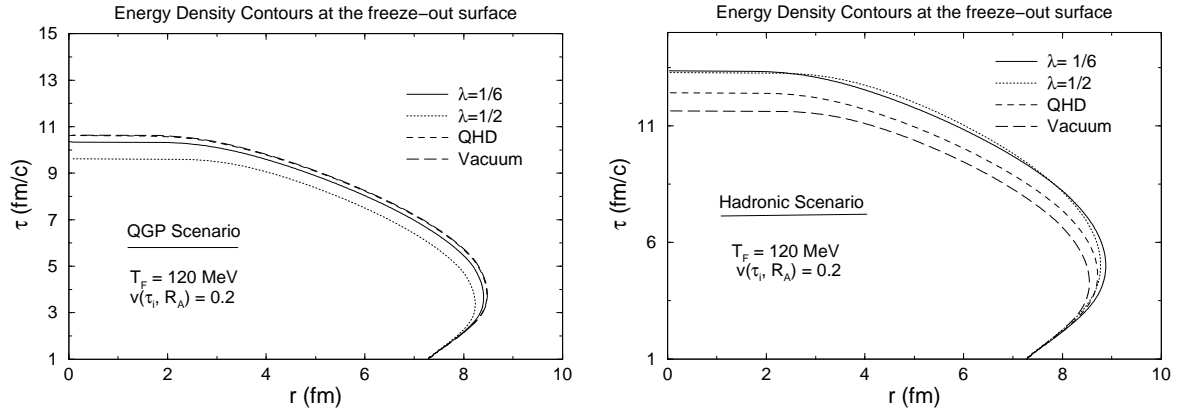


Figure 3: Same as fig. 2 for $v_0 = 0.2$.

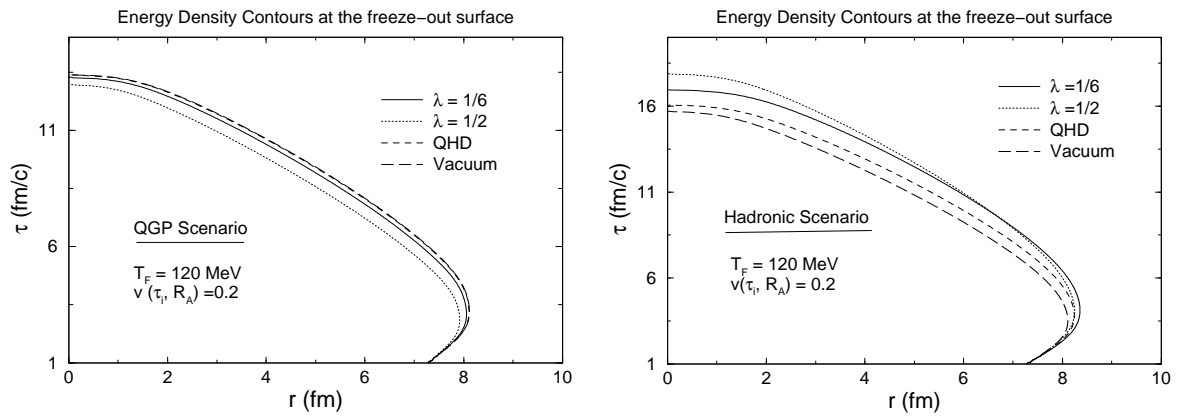


Figure 4: Same as fig. 2 with initial velocity profile of Eq. 6 for $v_0 = 0.2$.

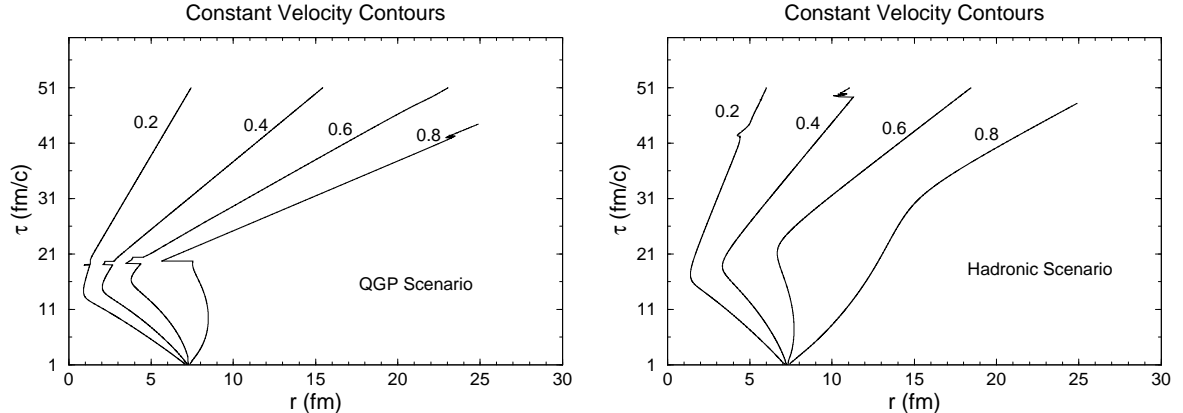


Figure 5: The constant velocity contours for the initial velocity profile of Eq. 5 with $v_0 = 0$. Left (Right): QGP (hadronic initial state for vacuum masses of hadrons).

$v_0 = 0.2$. It is clear that here the expansion is slower than the case in fig. 3, indicating that the radial velocity proportional to radial co-ordinate gives rise to stronger flow.

In fig. 5 we show the constant velocity contours for QGP and hadronic initial state when the medium effects on the hadrons are ignored. The initial velocity profile is given by Eq. 5 with $v_0 = 0$. Introduction of the medium effects does not change the qualitative behaviour of the contours as shown in fig. 6. In case of the QGP formation scenario the introduction of the medium effects has negligible effects on the space time evolution of the system (left panel of figs. 5 and 6). However, in case of the hadronic scenario (right panel of figs. 5 and 6) a visible quantitative change is evident. In fig. 7 the effects of non-zero initial radial velocity are shown, a quantitative difference with the results of the previous figure indicates a large transverse flow in this case.

Now we discuss the m_T spectra of pions and protons. We assume that pions and nucleons are in thermal equilibrium throughout the hydrodynamic evolution, and they freeze-out at a common temperature $T_F = 120$ MeV. We recall that there is no unique description so far for the p_T spectra of hadrons. In [26] it has been shown that the π^0 spectra of WA80 and WA98 can be reproduced by perturbative QCD calculation if the initial p_T broadening is taken into account. Wang [26] has argued that the high p_T π^0 spectra in central Pb + Pb collisions can not be due to collective flow. The p_T broadening in heavy ion collisions can also be described reasonably

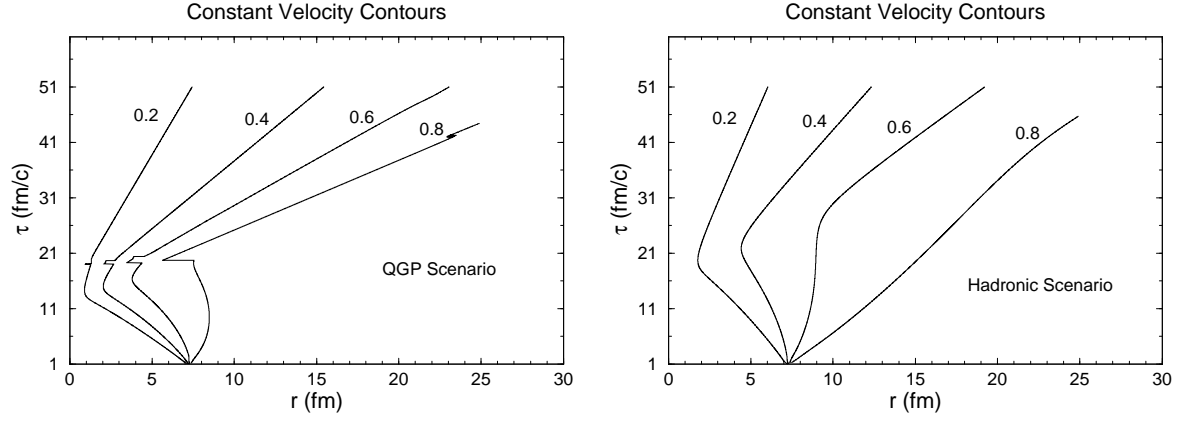


Figure 6: Same as fig. 5 for in-medium hadronic masses given by Eq. 15.

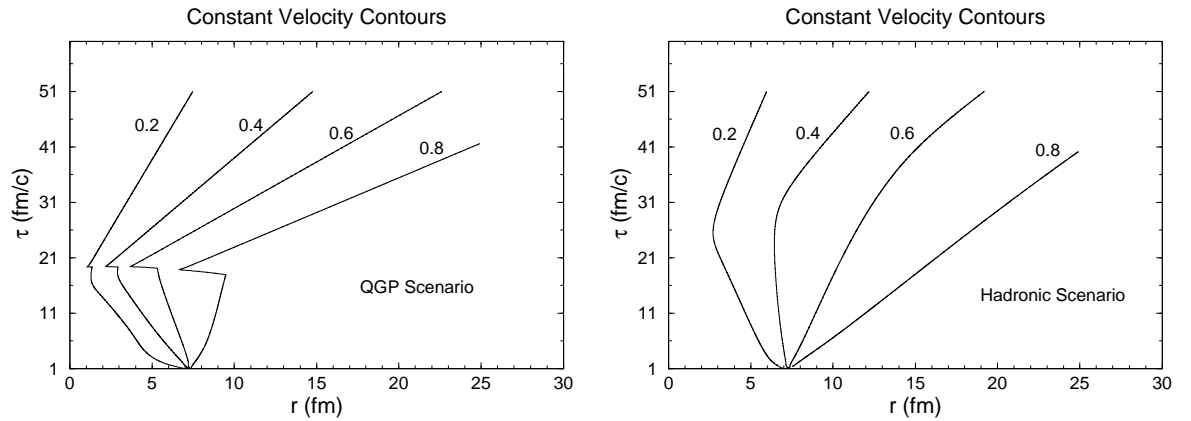


Figure 7: Same as fig. 6 for initial velocity profile of Eq. 6 with $v_0 = 0.2$.

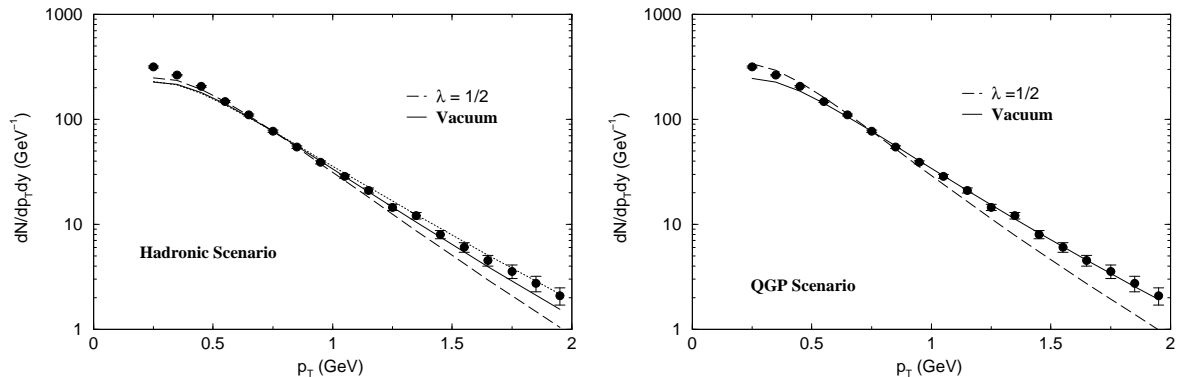


Figure 8: The p_T distribution of pions for Pb + Pb collisions at CERN SPS energies. Left (Right): hadronic (QGP) initial state. The hadronic masses vary according to Eq. 15 with $\lambda = 1/2$. The initial velocity profile is taken from Eq. 5 with $v_0 = 0$. The dotted curve in the left panel shows the pion spectra evaluated for the initial radial velocity of Eq. 5 with $v_0 = 0.2$.

well by a random walk model [27] where transverse flow effects are not required to reproduce the data. Recently it has been proposed that the p_T -broadening in high energy nuclear collisions can be generated by the Color Glass Condensate i.e. by the initial partonic phase formed after the collisions [28]. Keeping these possible scenarios of p_T broadening in mind we do not attempt to reproduce the absolute normalization of the high p_T part of the pion spectra by hydrodynamic flow. We rather concentrate on the effects of the EOS containing the in-medium mass modification of hadrons on the p_T spectra of pions and protons. We treat the normalization of pions and nucleons as parameters to be determined by the experimentally measured spectra. Negative hadrons and positive minus the negative are treated as pions and protons respectively. In fig. 8 the NA49 pion spectra is compared with both QGP and hadronic initial states. The hadrons (π^- and K^-) from the resonance decays (ρ and ϕ) are about 5% of the direct pions at $p_T \sim 500$ MeV and are therefore neglected here. Results for QGP (hadronic) initial state is displayed in the left (right) panel in fig. 8. Both the initial states describe the data reasonably well for low transverse momentum. In fig. 9 the similar results are shown for protons. The experimental spectra is well reproduced by the hadronic as well as QGP initial state. However, due to various uncertainties which are discussed above it is not possible to state which of the EOS is realized in such collisions.

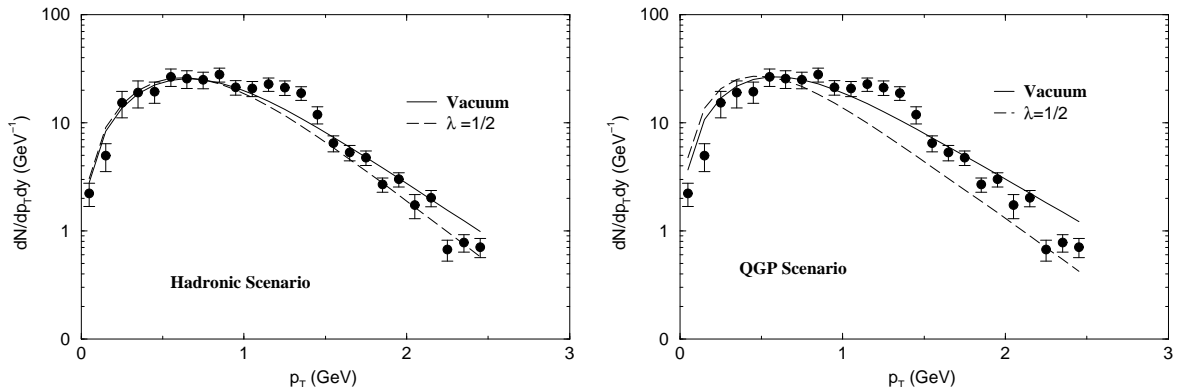


Figure 9: The p_T distribution of protons for Pb + Pb collisions at CERN SPS energies. Left (Right): hadronic (QGP) initial state. The initial velocity profile is taken from Eq. 5 with $v_0 = 0$. The hadronic masses vary according to Eq. 15 with $\lambda = 1/2$.

In fig. 10 the p_T spectra for negative hadrons at RHIC energies are shown for the same value of the freeze-out temperature (120 MeV) and the EOS as shown in fig. 1. The agreement of our calculation with the experimental data [29] is reasonably well. In this case a thermalized QGP with initial temperature ~ 300 MeV and thermalization time 0.5 fm/c is assumed.

4 Summary and discussions

We have solved the (3+1) dimensional hydrodynamical equations for QGP as well as hadronic initial states. The shift of hadronic masses at non-zero temperature are incorporated through the EOS. The FS is seen to be modified due to medium effects depending upon the magnitude of the shift in the hadronic masses. For a hadronic initial state in the universal scaling scenario (with the value of the exponent, $\lambda = 1/2$) the FS is larger compared to the case when no medium effects is considered. The difference in FS for QHD and vacuum scenario is negligible due to small mass shift in QHD near the freeze-out point. The pion and proton spectra is well reproduced by a hadronic initial state when the mass shift of hadrons are taken into account via the EOS. It is seen that the pion and proton spectra is well reproduced with the same equation of state, initial conditions and the freeze-out parameters which describe the WA98 [9] and the CERES/NA45 dilepton data [30], indicating a thermal source

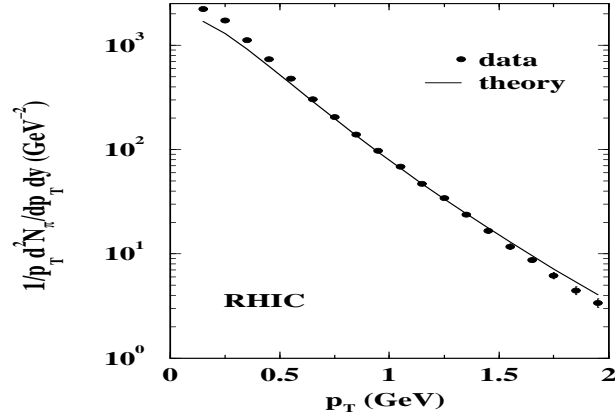


Figure 10: The p_T distribution of the pions at RHIC energies. The initial velocity profile is taken from Eq. 5 with $v_0 = 0$. The theoretical results are obtained for QGP initial state at a temperature 300 MeV.

of initial temperature ~ 200 MeV at CERN SPS energies.

Acknowledgement: J.A. would like to thank K. Redlich for encouragement on this work.

References

- [1] Proc. of the 15th Int. Conf. on Ultra-Relativistic Nucleus-Nucleus Collisions (Quark Matter-2001), January 15-20, 2001, The university of New York at Stony Brook and Brookhaven National Laboratory, USA, to be published in Nucl. Phys. A.
- [2] J. Cleymans and K. Redlich, Phys. Rev. **C 60** 054908 (1999).
- [3] P. Huovinen, P. F. Kolb, U. Heinz, P. V. Ruuskanen and S. A. Voloshin, Phys. Lett. **B 503** 58 (2001).
- [4] P. Braun-Munzinger, J. Stachel, J. P. Wessels and N. Xu, Phys. Lett. **B 365** 1 (1996).
- [5] D. Teaney, J. Lauret and E. V. Shuryak, nucl-th/0110037.
- [6] J. Sollfrank, P. Huovinen, M. Kataja, P. V. Ruuskanen, M. Prakash and R. Venugopalan, Phys. Rev. **C 55** 392 (1997).

- [7] G. Agakichiev *et al*, CERES Collaboration, Phys. Lett. **B 422**, 405 (1998); B. Lenkeit, Doctoral Thesis, Universitaet Heidelberg (1998).
- [8] R. Rapp and J. Wambach, Adv. Nucl. Phys. **25**, 1 (2000).
- [9] J. Alam, S. Sarkar, T. Hatsuda, T. K. Nayak and B. Sinha, Phys. Rev. C **63** 021901R (2001).
- [10] M. M. Aggarwal *et al.*, WA98 Collaboration, Phys. Rev. Lett. **85**, 3595 (2000).
- [11] H. Appelshäuser *et al.*, NA49 Collaboration, Phys. Rev. Lett. **82**, 2471 (1999).
- [12] J. D. Bjorken, Phys. Rev. **D 27**, 140 (1983).
- [13] H. von Gersdorff, M. Kataja, L. McLerran and P. V. Ruuskanen, Phys. Rev. **D 34**, 794 (1986).
- [14] U. Heinz, K. S. Lee and E. Schnedermann, in Quark Gluon Plasma, edited by R. C. Hwa, (World Scientific, Singapore 1992).
- [15] P. Braun-Munzinger, J. Stachel, J. P. Wessels and N. Xu, Phys. Lett. **B 365**, 1 (1996).
- [16] F. Cooper and G. Frye, Phys. Rev. **D 10** 186 (1974).
- [17] P. V. Ruuskanen, Acta Phys. Pol. **A 18**, 551 (1986).
- [18] J. P. Blaizot and J. Y. Ollitrault, in Quark Gluon Plasma, edited by R. C. Hwa, (World Scientific, Singapore 1992).
- [19] G. E. Brown and M. Rho, Phys. Rep. **269**, 333 (1996); Phys. Rev. Lett. **66** 2720 (1991).
- [20] T. Hatsuda, H. Shiomi and H. Kuwabara, Prog. Th. Phys. **95** 1009 (1996).
- [21] S. Sarkar, J. Alam, P. Roy, A. K. Dutt-Mazumder, B. Dutta-Roy and B. Sinha, Nucl. Phys. **A634**, 206 (1998); P. Roy, S. Sarkar, J. Alam and B. Sinha, Nucl. Phys. **A 653**, 277 (1999).
- [22] C. Song, P. W. Xia and C. M. Ko, Phys. Rev. **bf C52** 408 (1995).

- [23] S. Weinberg, Phys. Rev. Lett. **18** 507 (1967).
- [24] F. Karsch, hep-lat/0106019 (2000).
- [25] G. E. Brown, H. A. Bethe, A. D. Jackson and P. M. Pizzochero, Nucl. Phys. **A 560**, 1035 (1993).
- [26] X. N. Wang, Phys. Rev. Lett. **81**, 2655 (1998).
- [27] A. Leonidov, M. Nardi and H. Satz, Z. Phys. **C 74** 535 (1997); J. Alam, J. Cleymans, K. Redlich and H. Satz, nucl-th/9707042.
- [28] L. McLerran and J. Schaffner-Bielich, Phys. Lett. **B514** 29 (2001); J. Schaffner-Bielich, D. Kharzeev, L. McLerran and R. Venugopalan, nucl-th/0108048.
- [29] C. Adler et al. (STAR Collaboration), Phys. Rev. Lett. **87** 112303 (2001).
- [30] S. Sarkar, J. Alam and T. Hatsuda, nucl-th/0111032.